Improved illumination for vision-based defect inspection of highly reflective metal surface

Lin Li (栗 琳)[1,2*], Zhong Wang (王 仲)[1], Fangying Pei (裴芳莹)[1], and Xiangjun Wang (王向军)[1,2]

1. State Key Laboratory of Precision Measuring Technology and Instruments, Tianjin University, Tianjin 300072, China

2. MOEMS Education Ministry Key Laboratory, Tianjing University, Tianjin 300072, China

**Corresponding author: meiguiwuxinll@163.com*

Received May 28, 2012; accepted August 7, 2012; posted online January 21, 2013

Specular and strong reflections are the main problems encountered during part image defect inspection of shiny or highly reflective surfaces. In this letter, we propose an improved illumination method for defect inspection. A diffuse light source is designed based on the physics analysis of light reflection. The distribution of intensity is simulated according to a known model to verify the illumination uniformity of the source. Experiments show that defect expressivity when using the proposed illumination method has a better performance. The optical model is not only suitable for the defect detection of metal balls but also for the defect detection of planes and cylinders.

OCIS codes: 110.0110, 120.0120, 290.0290, 150.0150.

doi: 10.3788/COL201311.021102.

Inspection of highly-reflective surfaces is a frequently encountered problem[1−3]. A large number of shiny reflective surfaces need to be detected in modern manufactured products such as defect detection in steel balls, body-in-white spraying of cars, and surface inspection of polished abrasives. Specular reflection is generally produced on smooth surface. A reflected light with extremely high energy causes highlights when parallel rays are projected onto a smooth surface. The highlights cause technical problems during vision-based image acquisition. Technical problems arise because the surface defects submerge in the complicated background, which is attributed to local saturation in the recorded images.

Techniques have been developed to avoid or eliminate specular reflection. Seulin *et al.* proposed an approach using binary encoded structured light to dynamically scan the surface of metal parts; the image is recorded by a linear charged-coupled device (CCD)[4]. The defect is represented as a series of light spots in a dark background. In addition, structured light[1] of space encoding and color encoding[5] are developed. This kind of method is suitable for inspection of static objects. However, the method has low scanning speeds and limited scope of applications. Ng used ring light for the illumination of defects[6]. The ring light creates a highlighted circle that reveals surface defects clearly; a defect can be recognized when it is on the circle. Therefore, images of balls are acquired and defects are diagnosed through the variations in distance between the light source and the sphere. Obviously, ring light illumination and apparatus are not suitable for on-line detection because of its slow speed. A common method in dealing with specular reflection is the use of low-angle dark-field lighting technology[2]. This method reveals defects as bright spots in a dark background while the scattered light instead of the specular reflective light is recorded by a camera. Low-angle dark-field lighting technology is also suitable for planar surface detection. However, this method does not work well on free surfaces because shadows and brightness fluctuations increase image processing complexity. Leon reduced image highlights (a reduction of 65%[7]) by setting two polarizers: one in front of the light source, and the other in front of the camera under dark field lighting. Similarly, putting mirrored balls into the fluid medium weakens the intensity of reflected light[8]. The highlight still exists although the overall brightness of the image is reduced by these two methods. Valle *et al.* designed a nonplanar mirror model for highly reflective curved surfaces[9]. The reflected ray from the object surface, which is from the reflective ray of the mirror, is received by a CCD camera along its direction. Defects are dark whereas other regions of the surface are bright. However, the model is not reproducible because the mirror changes with the change in surface shape of the object. Other researchers study image highlights and shadows that are due to specular reflection with multi-image fusion technology[10,11] and multi-wavelength illumination technology[12].

The optical system is the most important part in visual detection, especially for imaging, image processing, and defect recognition[13]. A surface illumination model is investigated through the analysis of an optimum illumination method on a specular reflective object such as a sphere surface. A diffuse dome light emitting diode (LED) light is designed from a uniform point of view. The diffuse dome LED practically solves the defect imaging problems of mirrored surfaces. These problems include CCD saturation due to local image highlight and missing surface defect information because of the reflections of surrounding objects. This equipment provides clear defect information for image processing and defect recognition algorithm and improves system performance.

The bi-directional reflectance distribution function (BRDF) of an opaque surface patch is defined by how much light incident from each possible illumination direction is reflected in each possible observation or view direction[14]. As shown in Fig. 1, a surface patch with normal N is illuminated by a directional light source in direction S and observed by a viewer in direction V. θ_i and θ_r are the angles of S and V from the normal surface N; ϕ_I and ϕ_r are azimuthal angles from normal N. At least four angles (θ_i, ϕ_i, θ_r, and ϕ_r) in

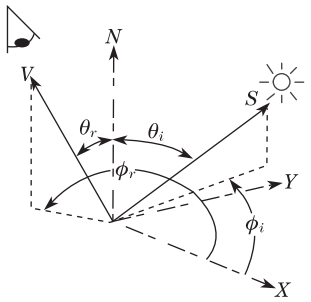

Fig. 1. Schematic diagram of BRDF.

a three-dimensional (3D) space are required to specify the direction of incident and reflected light. BRDF of a surface determines distribution of reflected light under any illumination.

Generally, reflections of light from surfaces are broadly classified into two categories: diffuse and specular. The former incident light is randomly reflected by the surface multiple times because of the inconsistent normal direction of each point. An ideal diffuse reflection or Lambertian has a constant BRDF no matter the direction of incident light.

$$f_{\rm d}(\theta_i,\ \phi_i;\ \theta_r,\ \phi_r) = \rho_{\rm d}/\pi, \tag{1}$$

where $\rho_{\rm d}$ is the diffuse proportion of the incident energy. The distribution of diffuse reflection is extremely wide, covering the entire hemisphere surface and the center of normal direction. The diffuse reflection of an ideal Lambertian surface does not change. Specular reflection occurs when incident light projects onto a smooth surface and reflects with the same angle as the incident light. The direction of the reflected light even in slightly rough metal surfaces depends on the direction of incident light and concentration of reflected energy beam. The BRDF of specular surface is expressed as

$$f_{\rm s}(\theta_i,\ \phi_i;\ \theta_r,\ \phi_r) = \frac{\delta(\cos\theta_i - \cos\theta_r)}{\sqrt{\cos\theta_i \cos\theta_r}}\delta(|\phi_r - \phi_i| - \pi). \tag{2}$$

A ward model is used in order to describe the BRDF of specular reflection, and is presented as[15]

$$f_{\rm s}(\theta_i,\ \phi_i;\ \theta_r,\ \phi_r) = \rho_{\rm s}\frac{1}{\sqrt{\cos\theta_i \cos\theta_r}}\frac{\exp(-\tan^2\delta/\alpha^2)}{4\pi\alpha^2}. \tag{3}$$

The total reflection f is the sum of the diffuse reflection and specular reflection:

$$f = f_{\rm d} + f_{\rm s}. \tag{4}$$

The diffuse reflection on a shiny metal surface is almost negligible compared with those of specular reflection. Therefore, the expression can be depicted similar to Eq. (3).

Scattered light is preferred for surface defects lighting. Two kinds of methods are needed to meet the condition. The first method sets the angle of the light source and the relative position between light source and camera. This is done to prevent direct reflected light from entering the camera. The second method aims to have a uniform distribution of scattering light by controlling the distribution of reflected light. The distribution of reflected light on a spherical surface is more complex than those of a planar surface. The complexity is caused by normal surface variations, which leads to direction changes of specular reflection along the surface. The reflected light, which is close to the light source, directly enters the CCD camera if the light source and the camera are in the same half sphere. The entrance of reflected light results in highlights on the surface. Regardless of the angle setting of the light source is, portions of reflected light will enter the lens to form highlights. Images of a shiny ball are taken under fluorescent lights and dark illumination as shown in Fig. 2. Dark illumination not only fails to eliminate highlights but also causes non-uniform brightness in the images.

A reflective light is designed in this letter through multi-scattering of LED rings to eliminate the reflections and highlights of surrounding objects. The design is derived from an integrating sphere, which has uniform scattering effects and is commonly used for photometric or radiometric measurements. Here, LED arrays are added as light sources and CCD cameras are used as emergent ray receivers. Parallel light from the three rings of the LED arrays enters the CCD camera after multiple reflections. The schematic diagram of the design is shown in Fig. 3.

A single LED can be regarded as a point light source because the radius of a LED is negligible compared with the irradiation distance. When the irradiation distance from a single LED to a plane is d, the irradiation of the plane is

$$E(r,\theta) = \frac{E_0(r)\cos^n\theta}{d^2}, \tag{5}$$

where $E_0(r)$ is the irradiance value from the LED point light source to a direct r linear point distance; $E(r,\theta)$ presents another irradiance value in polar coordinates (r,θ); n, which is generally greater than 1, is related to the half decay angle α provided by the manufacturers.

$$n = \frac{-\ln 2}{\ln(\cos\alpha)}. \tag{6}$$

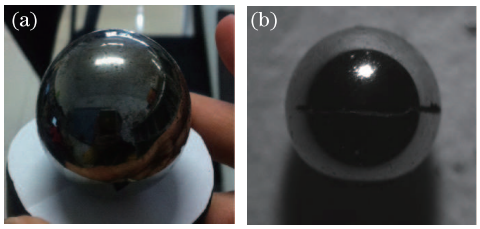

Fig. 2. Two shiny balls under different conditions: (a) fluorescent and (b) dark field illumination.

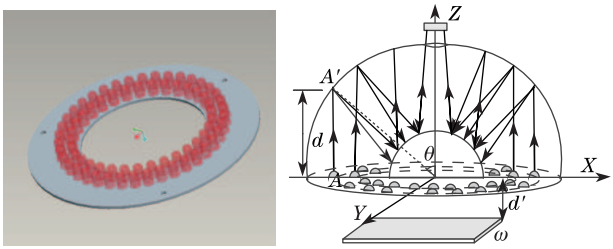

Fig. 3. Schematic diagram of homogeneous scattering based on a ring LED.

A single LED light source is set at A(x_0, y_0, 0) in Cartesian coordinates, as shown in Fig. 3.

$$\begin{cases} d = \sqrt{(x-x_0)^2 + (y-y_0)^2 + z^2} \\ \cos\theta = z/d \end{cases}. \tag{7}$$

The illumination of a single LED light source can be calculated in the diffuse dome by using Eq. (6).

$$E(x,y,z) = \frac{z^n E_0}{[(x-x_0)^2 + (y-y_0)^2 + z^2]^{(n+2)/2}}. \tag{8}$$

Similarly, the function of luminance distribution in the entire dome from the three LED arrays can be expressed as

$$\begin{cases} E(x,y,z) = z^n \sum_{i=0}^{m-1} \sum_{k=1}^{N} E_0 \left\{ \left[x - r_i \cos\left(\frac{2\pi n}{N}\right) \right]^2 \right. \\ \quad \left. + \left[y - r_i \sin\left(\frac{2\pi n}{N}\right) \right]^2 + z^2 \right\}^{-(n+2)/2} \\ x = R\sin\theta\cos\varphi \\ y = R\sin\theta\sin\varphi \\ z = R\cos\theta \end{cases}, \tag{9}$$

where m represents the number of rings, N is the number of LEDs in each ring; r is the radius of ring and R is the radius of the dome; θ and φ are parameters of the spherical coordinate system.

Luminance uniformity can be described as $U = E/E(\max)$. We set $m = 3$, $N = 30$, $R = 60$ mm, $r_0 = 31.875$ mm, $r_1 = 41.25$ mm, $r_2 = 50.625$ mm, $\theta \in [\pi/10, \pi/2]$, $\varphi \in [0, 2\pi]$, $\alpha = 30°$. A 3D description of the luminance uniformity of the diffuse reflection dome is shown in Fig. 4.

The diffuse reflection dome is approximately viewed as a Lambertian reflectance that expresses n as 1. The illumination distribution of the plane located below the light source can be calculated from the above BRDF when f is set at a constant value.

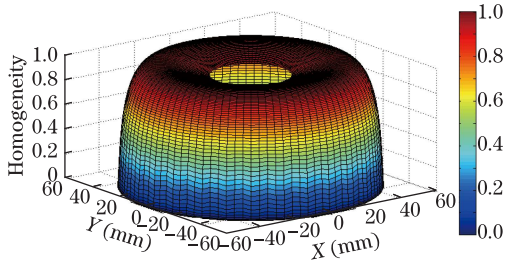

Fig. 4. Uniform distribution of luminance on diffuse hemisphere.

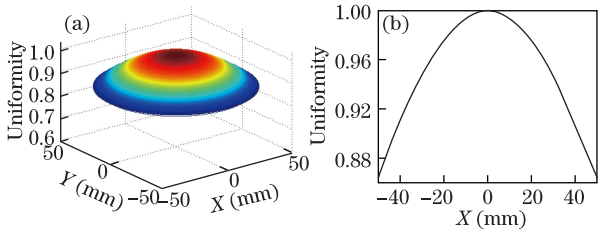

Fig. 5. Illuminance distribution of plane while $d' = 0.1$ m. (a) A 3D distribution and (b) an $x - y$ plane.

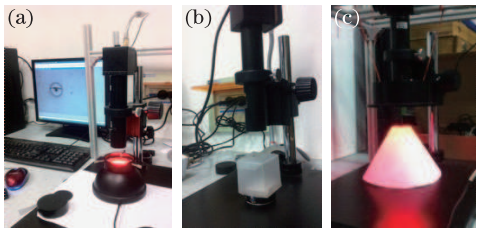

Fig. 6. Three lighting devices used to acquire steel ball images. (a) Light source designed in this letter, (b) diffuse light plus 78% transparent plastic box, and (c) ring light plus paper cone.

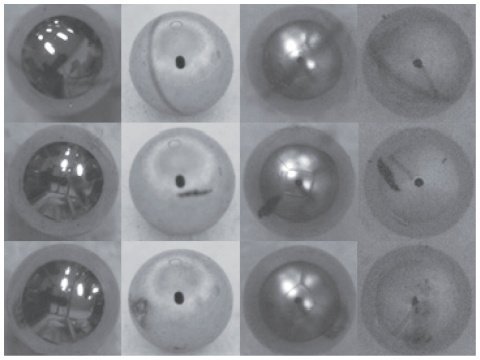

Fig. 7. Various defect images under different illuminations. The images gained under lighting in the second column are investigated in this letter.

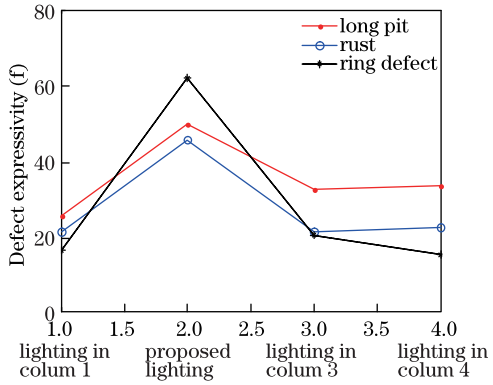

Fig. 8. Defect expressivity under four illuminations.

$$E' = E(x,y,z) \cdot f \cdot \cos\theta / d'^2. \tag{10}$$

The distribution of plane illumination when $d' =$ –0.1 m is shown in Fig. 5 with a uniformity of 86%. Simulation results reveal that the farther the detection plane from the light source, the better the uniformity. However, intensity is reduced because of the square of the distance on the denominator. Placing an internal diffuse light source prevents surface reflection when the detected object is a sphere. Thus, $d' > 0$.

The diffuse dome LED light source is developed in the manner described above. The inside surface of the dome which has an outer radius of 60 mm is coated with a mixture of barium sulfate, creamy white glue, and water at a certain ratio. High reflected steel balls of 1.5 mm in diameter are tested. The camera is a gray scale Weishi Corporation VS078FM with an array of 1 024×768 pixels and a 5x optical zoom lens. The acquisition unit with

different illuminations, except for fluorescent lamps, is shown in Fig. 6. The relevant defect images, which are recorded under four illuminations: a fluorescent lamps, a diffuse dome LED, a ball surrounded by a 78% plastic shade box, which was proposed by Do *et al.*[16], and a ring light source with a paper cone diffuse reflector, are respectively shown in the columns of Fig. 7. Three different defects are displayed in the rows from top to bottom.

Defect expressivity f denotes the capacity to reveal image defects and is defined as

$$f = (v - v'), \tag{11}$$

where ν is the averaged image intensity, and ν' is the averaged intensity in the region with defects. The results of f calculated in each image under the four light sources are shown in Fig. 8.

A maximum value of f is obtained under the light source proposed in this letter and under similar defects. The illumination in column 3 is better than the illumination in column 1. However, highlights and reflections in the images still exist. The illumination in column 4 has better diffuse reflection and uniformity. However, the transmission of light is so low that noise is very high. The light source used in this letter is intense enough to only need a single background. In addition, the light source is not affected by outside light. From a defect inspection perspective, the images taken under illumination in this letter are more suitable for defects detection. Both highlights and reflections are efficiently eliminated by this type of illumination. The result of template image subtraction is not affected although camera reflections exist in selected small regions. We note that implementing the proposed illumination in practice is difficult compared with the methods in column 3 or 4. Future studies will be concentrated on the practical implementation of high speed inspection. For example, a V-shaped rail, which extends into the center of the light source through two holes on the source dome, can be employed to feed balls.

Defect inspection is often conducted on a planar, cylindrical, or spherical surface. The illumination investigated in this letter is appropriate for highly reflective surfaces, and is capable of eliminating image highlights. Examples of planar and cylindrical surfaces are shown in Fig. 9. Ring light can be incorporated in the proposed illumination method for multi-mode inspection of defects such as defects associated with non-perfect spheres.

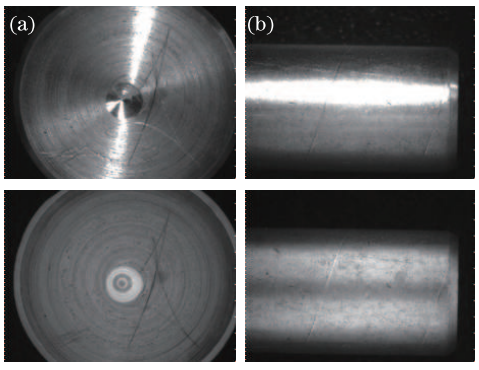

Fig. 9. Improved images on a metallic plane and cylinder. (a) A plane image is improved from top to bottom; (b) a cylinder image is improved from top to bottom.

In conclusion, defect inspection of the surface of industrial parts is often encountered in practical industrial inspection. A solution devoted to improving optical illumination is provided in this letter to deal with highlights and reflections on reflective and shiny surfaces. Experimental results show that the illumination designed in this letter has higher defect expressivity compared with other diffuse light sources. An extra experiment shows that the proposed illumination method works well on planar and cylindrical surfaces. However, this approach still needs to solve the problem of ball feeding to improve the speed of inspection. Further study is needed with more consideration for high speed inspection.

This work was supported by the CNC Machine Tools and Basic Manufacturing Equipment of the Important National Science and Technology Specific Project under Grant No. 2009ZX04014-092.

References

1. A. C. Sanderson, L. E.Weiss, and S. K. Nayar, IEEE Trans. Pattern Anal. Mach. Intell. **10,** 44 (1988).
2. C. Bakolias and A. K. Forrest, Proc. SPIE **3029,** 57 (1997).
3. B. G. Batchelor and P. F. Whelan, *Intelligent Vision Systems for Industry* (Springer-Verlag, London, 1997).
4. R. Seulin, N. Bonnot, F. Merienne, and P. Gorria, in *Proceedings of Conference on Machine Vision and 3-Dimensional Imaging Systems for Inspection and Metrology* 129 (2001).
5. A. Poularikas, *Digital Colour Imaging Handbook* (CRC Press, Boca Raton, 2003).
6. T. W. Ng, Meas. Sci. Technol. **18,** N73 (2007).
7. F. P. Leon, in *Proceedings of the European Symposium on Lasers and Optics in Manufacturing* 297 (1997).
8. Y. Wang, Y. Lin, D. Jia, Z. Zhang, and X. Liu, Bearing **5,** 37 (2010).
9. M. D. Valle, P. Gallina, and A. Gasparetto, IEEE/ASME Transactions on Mechatronics **8,** 309 (2003).
10. B. Liu, W. Liu, and J. Peng, Chin. Opt. Lett. **8,** 384 (2010).
11. Q. Miao, C. Shi, P. Xu, M. Yang, and Y. Shi, Chin. Opt. Lett. **9,** 041001 (2011).
12. K. Khalili and P. Webb, Machine Vision and Applications **18,** 73 (2007).
13. X. Qu, Y. He, F. Han, X. H. Zhao, and S. H. Ye, Acta Opt. Sin. **23,** 547 (2003) (in Chinese).
14. R. Dror, "Surface reflectance recognition and real-world illumination statistics", PhD. Thesis (Massachusetts Institute of Technology, 2002).
15. G. J. Ward, Comput. Graphics **26,** 265 (1992).
16. Y. Do, S. Lee, and Y. Kim, Meas. Sci. Technol. **22,** 107001 (2011).